ResearchGate

See discussions, stats, and author profiles for this publication at: https://www.researchgate.net/publication/278052129

Functionalized Clay Microparticles as Catalysts for Chemical Oscillators

ARTICLE *in* THE JOURNAL OF PHYSICAL CHEMISTRY C · OCTOBER 2014

Impact Factor: 4.77 · DOI: 10.1021/jp5032724

CITATION
1

READS
13

4 AUTHORS, INCLUDING:

Federico Rossi
Università degli Studi di Salerno
51 PUBLICATIONS **278** CITATIONS
SEE PROFILE

Sandra Ristori
University of Florence
84 PUBLICATIONS **957** CITATIONS
SEE PROFILE

Available from: Federico Rossi
Retrieved on: 30 January 2016

THE JOURNAL OF PHYSICAL CHEMISTRY C

Article

pubs.acs.org/JPCC

Functionalized Clay Microparticles as Catalysts for Chemical Oscillators

Federico Rossi,*[,†,∥] Sandra Ristori,[‡] Nadia Marchettini,[¶] and Ottorino L. Pantani[§,∥]

[†]Dipartimento di Chimica e Biologia, Università di Salerno, Via Giovanni Paolo II 132, 84084 Fisciano (SA), Italy

[‡]Dipartimento di Scienze della Terra & CSGI, Università degli Studi di Firenze, Via della Lastruccia, 3, 50019 Sesto Fiorentino, Italy

[¶]Department of Earth, Environmental and Physical Sciences-DEEP Sciences, Università di Siena, Pian dei Mantellini 44, 53100 Siena, Italy

[§]Dipartimento Scienze delle Produzioni Agroalimentari e dell'Ambiente, Università degli Studi di Firenze, P.zle Cascine 28, 50144 Firenze, Italy

Supporting Information

ABSTRACT: Catalytic micro- and nanoparticles are widely employed to study the global behavior of large networks of coupled chemical oscillators. In this paper, we present a new class of catalysts for the BZ oscillating reaction, based on the functionalization of natural inorganic materials (1:1 and 2:1 clays) through the sorption of the iron-complex ferroin on their surface. The small size of the clay basic units (diameter < 2 μm) and their colloidal nature make these particles interesting for studying systems having dimensions at the border between the nano- and the mesoscale. In the first part of this paper, we present the synthesis and the characterization of the ferroin-functionalized clay. We then show an extensive study on the oscillatory dynamics of the BZ reaction catalyzed by the clay. Through a direct comparison with a classical ferroin-catalyzed BZ system, we describe the modifications of the oscillation mechanisms induced by the new catalyst. Finally, we illustrate an application of the microparticles as a solid support for the study of synchronization in a network of independent chemical oscillators, showing that the diffusion of intermediate species can be fine-tuned through the stirring rate of the solution where the catalytic spots are soaked. The global system can be thus switched from a noncoupled to a coupled state.

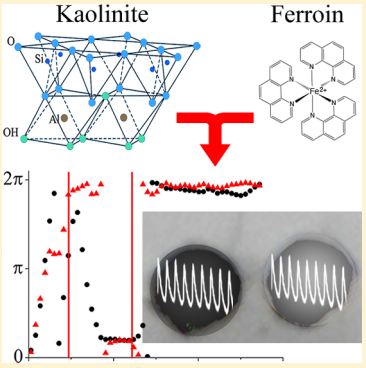

INTRODUCTION

Clays are intensively studied in many fields of science for their unique and interesting properties, such as the interaction with natural or xenobiotic molecules, which can be sorbed and transformed on their surfaces,[1−3] thus providing a large number of applications, from pharmacology[4] to material science and environmental chemistry.[5] Recently, self-assembling properties of clays have been exploited for the synthesis of a new type of vesicles, the so-called colloidosomes,[6] which raised great interest both for practical applications and for fundamental questions about the origin of life and prebiotic chemistry.[7−9] Self-assembling structures combined with self-organizing systems are known to yield the emergence of new dynamical behaviors at different length scales and provide clues on some phenomena of the biological realm (synchronization, communication, coupling, etc.).[10−14] In this paper, we introduce a new class of microparticles based on the functionalization of natural inorganic clays and with the ability to catalyze the self-organizing Belousov−Zhabotinsky (BZ) oscillating reaction. The small size of the particles and their resistance in acidic and oxidizing media allow their use for a large number of applications.

Clay minerals are the result of soil-forming processes, which start from the parent rock materials. They are found in the finer solid fraction of soil, and since their diameter is less than 2 μm, they have colloidal properties. Clays, which are mostly phyllosilicates, can be classified as 1:1 and 2:1 minerals, on the basis of their Si:Al ratio, with the latter characterized by a large specific surface (N_2 surface area about 30−100 $m^2\ g^{-1}$) and a high CEC (cation exchange capacity, 60−120 $cmol^+\ kg^{-1}$). Some 2:1 clays exhibit swelling properties in aqueous media (montmorillonites), due to the charge of the layers, which in turn originates from the isomorphous substitution of Al for Si or Mg/Ca for Al. When compared with 2:1, clay minerals 1:1 are characterized by low values of layer charge, small surface area (2−10 $cmol^+\ kg^{-1}$ and 10−20 $m^2\ g^{-1}$, respectively) and nonexpandability. These minerals are classified under the names of kaolinite or halloysite. All considered, clay surfaces are sites where molecules and cations can rest for some time and be recovered later by plants and micro-organisms, thus interfering or permitting information exchanges. For example, DNA fragments can be released after micro-organisms death and sorbed on clays, thus escaping or reducing the probability to be mineralized.[15] Those fragments

Received: April 2, 2014
Revised: September 23, 2014
Published: September 25, 2014

© 2014 American Chemical Society

dx.doi.org/10.1021/jp5032724 | J. Phys. Chem. C 2014, 118, 24389−24396

can later be recovered by new micro-organisms, which in turn can inherit some new functional traits (e.g., enzyme production) from past populations. Such processes were probably fundamental for the origin of life and its evolution on Earth.[16]

Here, the Fe(II) 1−10-*o*-phenantroline complex (ferroin), a chromogenic catalyst for the BZ reaction, was loaded on the surface of 1:1 and 2:1 homoionic clays, to form a new type of catalytic microparticles. A number of works have already dealt with the confinement of BZ catalysts on synthetic solid substrates (e.g., ion exchange resins,[17] glasses,[18] and porcelain,[19] but, as far as the authors are aware, no studies have been undertaken in the presence of natural inorganic materials). Ferroin-loaded clays were used in two types of experiments: (i) in a bulk system, to study the oscillatory dynamics of a BZ system catalyzed by the functionalized clays and (ii) as a catalytic substrates in a lattice of independent oscillators to study their global coupling and synchronization.

MATERIALS AND METHODS

Clay Preparation and Characterization. The behavior of BZ reaction in the presence of several clays saturated with different cations was explored and monitored. Among these, kaolinite made homoionic to Ca^{2+} ion (Ca-Kao) turned out to be the most stable in the acidic and oxidizing BZ environment; therefore, only these results are reported in the following. Complementary data on other homoionic clays can be found in the Supporting Information.

Kaolinite (Zettlitz, Czechoslovakia, CEC ∼10 $cmol^+ kg^{-1}$) was made homoioic to Ca^{2+} by treating the <2 μm fraction (separated by sedimentation) with a 1 N solution of $CaCl_2$ for three times. The excess of $CaCl_2$ was then removed by washing with double distilled H_2O until a negative $AgNO_3$ test was obtained. The clay was recovered as pellet after centrifugation at 5500*g* at 20 °C for 20 min. Water was finally added to reach [Ca-Kao] = 10 mg mL^{-1}, and the suspension was stored at 4 °C until used. Ca-Kao was subsequently saturated with ferroin (Ferr-Kao) as follows: 10 mL of 25 mM ferroin solution were added to 4 mL of clay suspension, kept in contact for 2 h and then washed as described above, until no red color was detectable in the supernatants (7−9 washings). Water was then added to reach a final volume of 4 mL.

The structural properties of Ferr-Kao and Ca-Kao as well as the ferroin location in the colloidal particles were investigated by X-ray diffraction (XRD), small angle X-ray scattering (SAXS), extended X-ray absorption fine structure (EXAFS), and X-ray absorption near edge structure (XANES). The patterns obtained from these X-ray techniques are reported in X-ray characterization of the Supporting Information and are discussed in Results and Discussion.

The amount of ferroin sorbed on the clay was determined by measuring the C and N content in Ferr-Kao by flash combustion, with Ca-Kao as the blank. The average quantity of ferroin was found to be 35 ± 0.1 nmol for 1 mg of clay (details in Elemental analysis of the Supporting Information).

Bulk Experiments. Experiments in bulk solution (batch) were run to evaluate the effects of clay on the oscillatory dynamics of the BZ reaction. In particular, a system containing the Ferr-Kao catalyst was compared with a classical BZ reaction containing the same initial concentration of ferroin. Moreover, in order to understand the influence of the clay on the oscillation parameters, several systems catalyzed by Ferr-Kao were studied in the presence of increasing amount of Ca-Kao. Optimal conditions for sustained oscillations were obtained with the concentrations reported in Table 1.

Table 1. Experimental Conditions for Bulk Experiments

chemical	concentration
Malonic acid (MA)	0.03 M
H_2SO_4	0.31 M
$NaBrO_3$	0.12 M
ferroin	1.8×10^{-4} M
Ferr-Kao	5 g L^{-1}
Ca-Kao	from 0 to 5.1 g L^{-1}

Commercial-grade reactants from Sigma-Aldrich, malonic acid (MA), $NaBrO_3$, ferroin (Ferr), and H_2SO_4 were used without further purification. Deionized water from reverse osmosis (Elga, model Option 3), having a resistivity higher than 1 MΩ cm^{-1}, was used to prepare all solutions.

Oscillations were monitored by means of a potentiometer (AMEL 2335) equipped with a platinum electrode as indicator and a Hg_2SO_4 electrode as reference. The reference was immersed in a KNO_3 solution connected to the BZ solution through a saline bridge. All experiments were run at room temperature; data acquisition was started a few seconds before adding H_2SO_4 as the last reactant. The stirring rate was set to 200 and 500 rpm for BZ-water and BZ-clay, respectively.

Arrays of BZ-Clay Oscillators. Figure 1 shows a simple sketch of the setup used for experiments on synchronization.

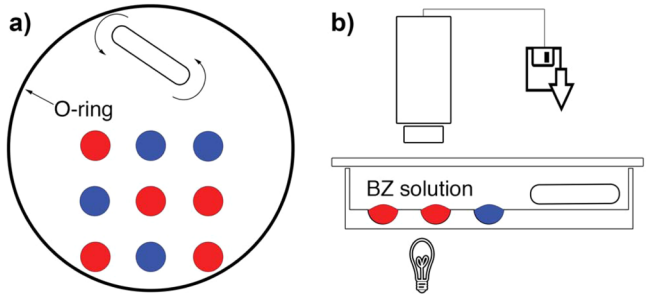

Figure 1. Sketch of the experimental setup used to study the synchronization of independent Ferr-Kao catalyzed BZ oscillators. (a) Top view and (b) side view.

Different lattices with a variable number of elements (1 mm diameter, centers 1.3 mm apart from each other) were carved in microscope glasses by using a precision drill press equipped with a spherical bit. The lattices were encircled by a silicon O-ring (diameter 20−25 mm; cross-sectional thickness 1.5−2 mm), which was glued to the glass with a few drops of cyanoacrilate. 7−8 μL of Ferr-Kao at a concentration of 5 g L^{-1} were deposited on the hemispherical wells. Water was subsequently evaporated by gently warming the glass, so that in each hole there were approximately 37.5 μg of clay loaded with a ferroin amount of about 1.3 nmol. One milliliter of a BZ solution with the initial concentrations of reactants reported in Table 1 and without the catalyst was dropped on the lattice, such that all the elements were completely immersed in the solution. A magnetic stirring bar was placed within the O-ring and beside to the lattice, and the reactors were sealed with a glass placed on top of the O-ring to prevent evaporation. The stirring rate was varied in the range of 200−500 rpm. In few experiments, some small flakes detached from the lattice when

dx.doi.org/10.1021/jp5032724 | J. Phys. Chem. C 2014, 118, 24389−24396

the system was mixed at the highest stirring rate; however, no significant influence on the dynamical behavior of the system was detected. The reactor was illuminated from below with a LED light source, while a CCD camera (PiXeLink PL-A774), equipped with a close focus zoom 10× (Edmund optics) and a band-pass interference filter (Edmund optics, λ = 510 nm), was placed above the sample and connected to a PC for frames acquisition.

Space-time (ST) plots for studying the oscillatory dynamics of each element of the lattice were built by cutting thin slices (1 pixel-thick) from the same region of every frame of the recorded sequences and pasting them sequentially in a new image. Every pixel on the vertical time axis represents the image capture sampling time (1 s), and the space axis represents the actual space captured by the camera. Time series of the BZ runs were built from the images by extracting the gray level of every pixel, with the highest values (brightest in the images) corresponding to the oxidized form of the catalyst (Fe^{III}–Kao).

RESULTS AND DISCUSSION

Ferr-Kao as New Catalyst for the BZ Reaction. As mentioned in the introduction, clay surfaces are able to adsorb a variety of chemical species, thus modifying their concentration in solution, as well as their physicochemical properties and reactivity. For instance, 1,10-*o*-phenantroline interacts with clays and iron oxides by forming clusters of 3.5 molecules in octahedral arrangement,[20] a geometry resembling both the clay lattice and the ferroin structure. This cluster is then sorbed onto the mineral surfaces. The interaction of ferroin with hectorite, a 2:1 clay mineral, is reported to modify the redox properties of the ferroin/ferriin couple.[21]

In this work, SAXS and XRD experiments performed on kaolinite made homoionic with mono-, di-, and trivalent cations allowed for inference that ferroin is located on the clay surface. In fact, SAXS diagrams (Figure 3 of the Supporting Information) showed that the colloidal grains of kaolinite grew in the presence of ferroin, irrespectively of the saturating cation. This effect was attributed to a charge screening exerted by the hydrophobic moieties of the ferroin ligands. Moreover, the XRD patterns did not show any variation in the interlayer distance of the clay after ferroin sorption (Figure 1 of the Supporting Information). XANES and EXAFS diagrams (Figure 2 of the Supporting Information) suggested that ferroin undergoes some modifications when in the sorbed state. Unfortunately traces of Fe oxides in the natural materials interfered with the measurements and did not allow for the collection of more detailed information.

The new complex Ferr-Kao maintains the catalytic properties of ferroin together with a remarkable chemical stability even in the strongly acidic and oxidizing BZ environment; these facts led us to consider Ferr-Kao as a new catalyst for the BZ system. We characterized its redox potential by means of pulsed voltammetric measurements (see Figure 4 of the Supporting Information for details), evidencing a substantial potential decrease from 0.75 to 0.57 V in 1 M H_2SO_4 with respect to a reference (Ag/AgCl electrode). This fact indicates that clay-bound ferroin molecules are more easily oxidized than their free counterparts, thus impacting the oscillation parameters as shown in Results and Discussion.

At the end of each BZ run, the catalyst Ferr-Kao is no longer reactive. However, the original catalytic activity of the complex could be simply restored by reloading the clay with fresh ferroin, as described in the experimental section. This behavior indicates the stability of this mineral matrix which is also able to retain its original CEC. The loss of catalytic activity during the oscillatory cycles of the BZ reaction was likely due to the cleavage of ferroin in acidic environments, according to the reaction.

$$Fe(phen)_3^{n+} + H^+ \overset{K_d}{\rightarrow} Fe^{n+} + 3PhenH^+ n = 2, 3 \qquad (1)$$

K_d was measured in the experimental conditions reported in Table 1, both for the ferroin in water solution (1.98×10^{-5}) and for Ferr-Kao (1.2×10^{-3} s^{-1}). An increase of almost 2 orders of magnitude was found for Ferr-Kao (see Decomposition of the Supporting Information for details). Therefore, the association of the *o*-phenantroline with the kaolinite accelerated the decomposition of ferroin. This phenomenon could be due to the sorption of H^+ on clay surfaces. Molecules on clay surfaces can thus experience lower pHs than those in solution.[22]

Chemical Oscillations. In order to understand the behavior of the BZ reaction catalyzed by the complex Ferr-Kao, we had to separate the effects of the new coordination sphere of ferroin from the effects that the clay surfaces exert on the BZ reagents and intermediates. In this respect, we first compared a classical BZ reaction with a system containing Ferr-Kao at 5 g L^{-1}, so that the catalyst concentration was constant in both systems (1.8×10^{-4} M). We then progressively increased the concentration of Ca-Kao in the solution containing a constant level of Ferr-Kao: this strategy allowed for the discrimination between the contribution of the different redox potentials and the influence of the sorption of species on clay surfaces.

Figure 2 compares the time series of the BZ reaction performed in water and in clay-containing systems. In pure water, no induction period (IP) was observed, as it usually

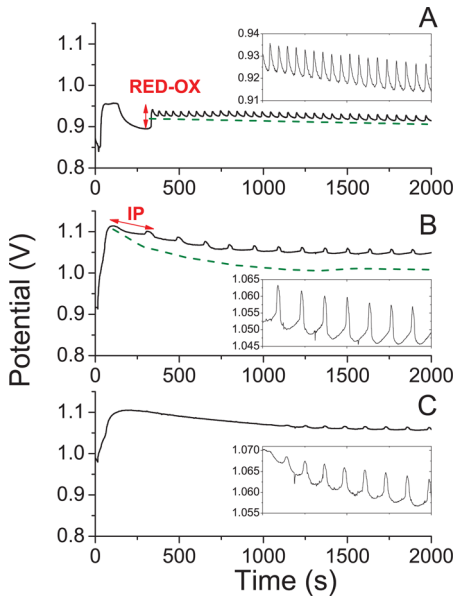

Figure 2. Time series of three different BZ systems: (A) [ferroin] = 1.8×10^{-4} M; (B) [Ferr-Kao] = 5 g L^{-1}; (C) [Ferr-Kao] = 5 g L^{-1} and [Ca-Kao] = 5.1 g L^{-1}. The green dashed lines in (A and B) represent the trend of the mean oscillation potential calculated by means of the Savitzky-Golay algorithm;[23] they have been offset from the time series for the sake of clarity. Insets show a magnification of the range 1000–2000 s for each time series.

dx.doi.org/10.1021/jp5032724 | J. Phys. Chem. C 2014, 118, 24389–24396

happens for ferroin catalyzed BZ systems.[24,25] The system only showed a first prolonged oscillation where ferroin underwent a quasi-quantitative redox reaction (indicated as RED-OX in the panel A of Figure 2). When ferroin was replaced by Ferr-Kao as catalyst (Figure 2 B), this first quantitative oscillation was replaced by an interval with no oscillation, reminiscent of the induction period typically observed in the cerium-catalyzed BZ system.[25] The IP was dramatically more evident when Ca-Kao was added to the reactive solution in the presence of Ferr-Kao, as illustrated in the panel C of Figure 2 where [Ca-Kao] = 5.1 g L^{-1} (i.e., the maximum concentration of clay used in our experiments). Another difference among the classical ferroin-catalyzed BZ reaction and those containing clay was the pronounced decrease of the mean oscillation potential, as highlighted by green dashed lines reported in panels A and B of Figure 2. These lines pass through the average values between maxima and minima of each oscillatory cycle and have been shifted from the potential traces for the sake of clarity.

In addition to the IP, the dependence of the oscillation period, τ_m, and the oscillation amplitude, h_m, were also investigated as a function of Ca-Kao concentration (Figure 3), increasing from 0 to 5.1 g L^{-1} in a system with [Ferr-Kao] = 5 g L^{-1}.

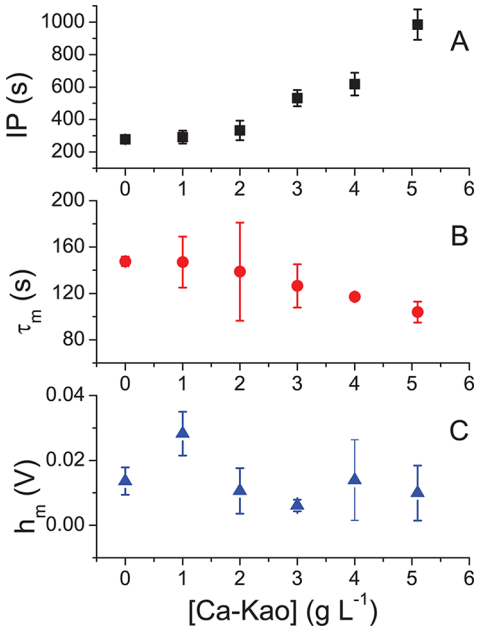

Figure 3. Relevant parameters of the BZ-clay reactions as a function of the Ca-Kao concentration when [Ferr-Kao] = 5 g L^{-1}.

The parameter most affected by Ca-Kao was the IP, which was not observed in pure water and changed from ~250 to ~1000 s as the [Ca-Kao] was increased from 0 to 5.1 g L^{-1}, while τ_m slightly diminished and h_m was not heavily influenced by the Ca-Kao concentration (Figure 3, panels B and C, respectively).

Table 2 summarizes the main differences among the classical BZ reaction without clays and the systems containing Ferr-Kao and/or Ca-Kao at the largest concentration.

Discussion. Insights on the observed behavior were obtained by comparing the properties of reactants in water and in association with clay. The redox potential and degradation rate of ferroin as well as the reactivity/availability of MA were the main features to be taken into account. For the clarity of the discussion, it is worth recalling the steps which mostly influence the oscillatory parameters monitored in the course of the reaction:

(1) the IP depends on the amount of brominated organic substrates accumulated before the onset of the oscillatory cycles.[25−27]

$$\mathrm{MA} \rightleftharpoons \mathrm{enol} \quad (2)$$

$$\mathrm{enol} + \mathrm{Br_2} \rightarrow \mathrm{BrMA} \quad (3)$$

(2) Bromination of MA mainly depends on the reaction between bromine and the enol form of MA itself, as shown in the reactions 2 and 3.

(3) τ_m and h_m depend on the process 4, as described in the FKN model,[28,29] where the reduction of the catalyst and the regeneration of Br^- reset the cycle.

$$2\mathrm{Fe(phen)_3^{3+}} + \mathrm{MA} + \mathrm{BrMA} \rightarrow f\,\mathrm{Br^-} + \text{other products} \quad (4)$$

being f a stoichiometric factor which depends on the experimental conditions.

(4) The total number of the oscillatory cycles and the mean oscillation potential may depend, in general, both on the concentration of the catalyst and on the concentration of the organic substrate.[24,28]

The appearance of an IP in the ferroin-catalyzed BZ system has also been observed in a zwitterionic micellar medium, where it was due to the sequestration of Br_2 by the micelles.[30,31] Following the approach of previous work, we reinvestigated the mechanism of bromination of the malonic acid (reactions 2 and 3; see Malonic acid bromination of the Supporting Information for details) by measuring the absorbance of Br_2 at 400 nm as a function of time, in a solution where the reactants concentration is such that the bromination process follows a zero-order kinetics. Results showed that the enolization rate constant did not markedly change, increasing from 2.19 to 2.78 × 10^{-3} s^{-1} for the water and the clay system, respectively. Therefore, being Br_2, the limiting reactant of the bromination process, we can suppose that its concentration and/or reactivity is not modified by the presence of clay.

Table 2. Relevant Oscillatory Parameters for the BZ-Water System ([Ferr] = 1.8 × 10^{-4} M) and for the BZ-Clay System ([Ferr-Kao] = 5 g L^{-1}, Corresponding to [Ferr] = 1.8 × 10^{-4}) at [Ca-Kao] = 0 and 5 g L^{-1}

	BZ-water [Ferr] = 1.8 × 10^{-4} M	BZ-clay [Ca-Kao] = 0 g L^{-1}	BZ-clay [Ca-Kao] = 5 g L^{-1}
induction period (IP), s	not present	279 ± 10	984 ± 94
oscillation period (τ_m), s	60 ± 15	148 ± 9	115 ± 9
amplitude (h_m), V	1.1 ± 0.01 × 10^{-2}	6 ± 1 × 10^{-3}	1 ± 0.8 × 10^{-2}
oscillatory cycles, n	~ 40	~ 20	~ 20

dx.doi.org/10.1021/jp5032724 | J. Phys. Chem. C 2014, 118, 24389−24396

The role of MA was investigated by changing its initial concentration at a fixed Ca-Kao content (1 g L^{-1}). The results are reported in Table 3 and demonstrated that MA and BrMA

Table 3. In the Presence of [Ca-Kao] = 1 g L^{-1}, the Induction Period (IP) is Shortened by Increasing the Initial Concentration of MA

[MA] mol L^{-1}	I.P.
0.006	~330
0.03	~290
0.1	~270
0.6	~220

are the key species in determining the IP duration. In fact, organic acids are known to interact with clay surfaces and to be absorbed on them. Sorption influences the reactivity of the organic molecules because of sterical reasons and because some chemical groups can be engaged in bonds with clay surfaces or saturating cations. This was shown to happen, in particular, for MA, whose sorption on kaolinite occurs through hydrogen bonds with hydroxyl and/or siloxanic groups of the clay itself.[32] Moreover, other studies on dicarboxylic acids showed that the amount of acid sorbed increases both with the length of the aliphatic chain among the two carboxylic groups and with lower pHs of the solution, suggesting that a hydrophopic effect between the associated acid and the siloxanic surfaces may also be responsible for the sorption.[33,34] We therefore measured the sorption of MA on kaolinite in experimental conditions used for the BZ reactions; in particular, we investigated by means of ionic chromatography (see the section Malonic acid sorption on Ca-kaolinite of the Supporting Information for details) the equilibrium.

$$MA_{solution} + CaKao \overset{K}{\rightleftharpoons} CaKao - MA_{sorbed}$$

to find a sorption constant $K = 10.5 \pm 0.3$ mol^{-1} L.

The variation in the values of τ_m and h_m could be ascribed to the decrease of the catalyst redox potential, which pushes the system into a more oxidized state, thus shifting reaction 4 to the left. This fact implies a shorter oscillation period and a decreasing oscillation amplitude.[24,29] Finally, the shorter lifespan of the reaction and a faster decay of the mean oscillation potential can be both accounted to the faster decomposition of the ferroin when embedded in the kaolinite.

In order to check whether the aforementioned modifications to the various single mechanisms could influence the global dynamics of the chemical oscillator, some computer simulations were run by using the software CO.PA.SI.[35] The model used was a standard set for the ferroin-catalyzed BZ systems,[36] as reported in the Supporting Information, together with the values for the constants of each reaction, also including the reactions for MA bromination (reactions 2 and 3).[30]

Moreover, we included in our model the reaction 1, which is generally neglected because of its slow rate. The decomposition products, the aqua-ion $Fe^{n+}\cdot 6H_2O$ and the ligand $PhenH^+$, are not included in the model since they are likely to be adsorbed on the clay surface[20] and, in any case, they do not interact with the BZ reaction mechanisms.[37]

Finally, we included two reactions to account for the partition equilibrium of the organic substrates between clay surfaces and solution.

$$Ca - Kao + MA \leftrightarrow P_1 \quad (5)$$

$$Ca - Kao + BrMA \leftrightarrow P_2 \quad (6)$$

The reaction 7 is the determinant step of the process 4; therefore, we changed the forward kinetic constant to account for the modification of the redox potential.

$$Fe(phen)_3^{3+} + BrCH(COOH)_2 \rightleftharpoons Fe(phen)_3^{2+} + {}^{\bullet}CBr(COOH)_2 + H^+ \quad (7)$$

All the new and changed kinetic constants are listed in Table 4. The values for reactions 2, 1, and 5 have been determined in

Table 4. Constants Used in Simulations

reaction	BZ− H_2O	BZ−Clays
7	50 mol^{-1} L s^{-1}	32 mol^{-1} L s^{-1}
2	2.19×10^{-3} s^{-1}	2.78×10^{-3} s^{-1}
1	1.98×10^{-5} s^{-1}	1.2×10^{-3} s^{-1}
5	0 mol^{-1} L s^{-1}	11 mol^{-1} L
6	0 mol^{-1} L s^{-1}	11 mol^{-1} L

this work. The value for 6 was assumed to be equal to 5, while the value for the reaction 7 was tuned to fit the simulations to the experimental data.

Figure 4 shows the simulated time series of a classic BZ reaction in water (panel A) and a system catalyzed by Ferr-Kao where [Ca-Kao] = 0 g L^{-1} (panel B). The comparison between these two time series revealed that the basic modifications induced by the substitution of ferroin with Ferr-Kao as the catalyst are qualitatively well-reproduced. In fact, the

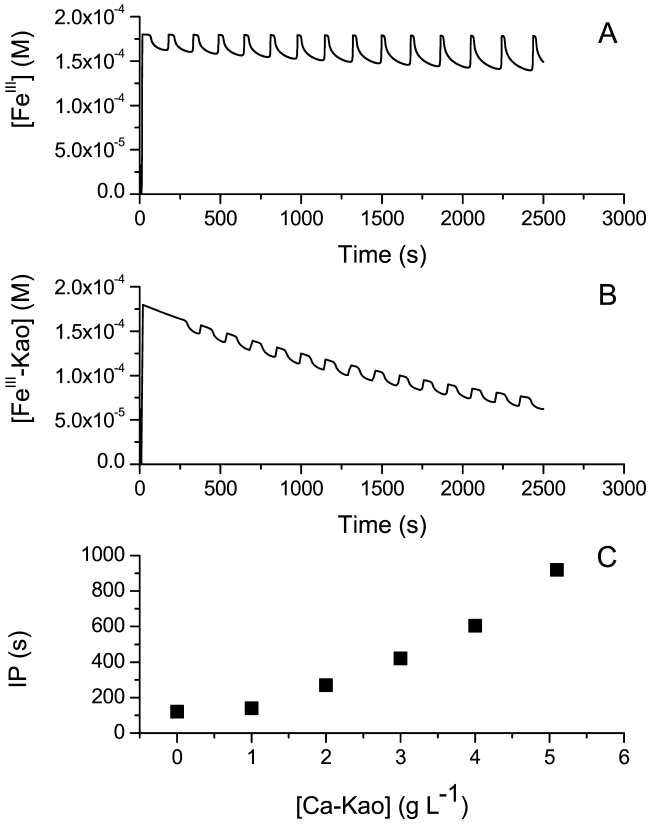

Figure 4. Numerical simulations of the BZ systems. (A) Classic BZ reaction in water. (B) Ferr-Kao-catalyzed BZ reaction in the presence of [Ca-Kao] = 0 g L^{-1}. (C) Behavior of the IP upon an increasing [Ca-Kao] in solution.

dx.doi.org/10.1021/jp5032724 | J. Phys. Chem. C 2014, 118, 24389−24396

appearance of an IP, the fast decay of the mean oscillation potential, and the slight decrease of τ_m and h_m, certainly account for the experimental observations already reported in Figure 3. Figure 4C shows the direct relationship between IP length and Ca-Kao concentration. Again, simulations show a behavior in line with the experimental results.

Using Clays to Study the Global Behavior of Coupled BZ Oscillators. The new catalyst Ferr-Kao can be used in those applications requiring a solid support for chemical oscillators. Examples are those systems where multiple single oscillators need to be separated from neighbors, such as in the study of the synchronization dynamics in complex networks of oscillating droplets[38,39] or liposomes.[40] In previous works, Taylor et al.[41] loaded ion-exchange resin beads with the ferroin and let them float freely in a BZ solution to study the collective behavior of a large population of independent chemical oscillators. Similarly, Fukuda et al.[42] fixed catalyst-loaded beads to a solid support, for studying the propagation of waves throughout a lattice immersed in a BZ solution. Smith et al.[43] synthesized a ruthenium-functionalized hydrogel, which can be stamped on gelatin films to create arrays or lattices of coupled oscillators.

Here we show how functionalized clays can be employed for similar studies; in particular, we investigated the global synchronization dynamics of a 6-elements (2 × 3) lattice (Figure 5a), as a function of the stirring rate. Figure 5b shows the ST plot of the system during the full evolution of the synchronization process. In the dark areas, the catalyst is in its reduced form (Fe^{II}–Kao), while bright flashes correspond to the autocatalytic oxidation to Fe^{III}–Kao. In the absence of stirring, after an initial IP (~150 s), each element of the lattice begins to oscillate approximately at the same time, as it can be seen in the ST plot and in the time series reported in Figure 5c.

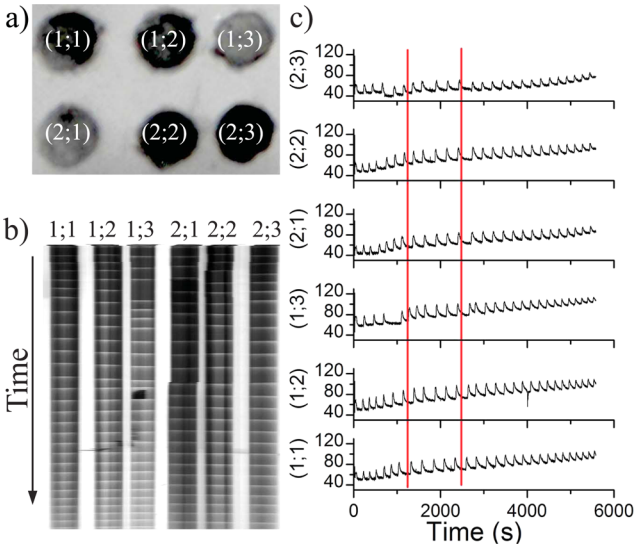

Figure 5. Global behavior of a 2 × 3 lattice where single Ferr-Kao oscillators are globally coupled through a BZ solution. (a) The 6 elements of the lattice (i; j) in different oxidation states, (1;3) and (2;1) oxidized (bright color) and all the rest reduced (dark color). (b) ST plot of each element of the lattice, total time 5500 s. (c) Time series of the oscillatory dynamics of each element of the lattice, extracted from the ST plot. Vertical red lines in (c) indicate the time at which the stirring rate was varied, from zero to a low stirring rate (left bar) and finally to a high stirring rate (right bar).

This indicates that, even though small differences in the amount of catalyst in the single elements can be possible, the chemicals are homogeneously distributed and initial conditions are roughly the same for all the independent oscillators. However, after the first global oscillation, the oscillatory dynamics of each element evolves independently with characteristic parameters dictated by the local conditions only. The distance among the spots is, in fact, large enough to avoid coupling mediated by diffusion of the key intermediates, such as the activator $HBrO_2$ and/or the inhibitor Br^-.[42] A communication path among the oscillators can be established by stirring the solution and favoring the homogenization of the system. A mild stirring was turned on at about 1000 s and then increased at about 2500 s. Both the ST plot and the time series show a progressive evolution toward synchronization after the global coupling of oscillators, similar to what was already observed for resin bead systems.[41,44] The synchronization dynamics can be highlighted by the time-evolution of the phase difference ($\Delta\phi_{ij}$) between couples of elements and by the time-evolution of the period (τ) of each single oscillator.

As an example, Figure 6a reports the evolution of $\Delta\phi_{ij} = (\phi_i - \phi_j) \mathrm{mod}(2\pi)$ for two couples of the lattice: (2;1)-(2;2) and (2;2)-(2;3). Phase values were calculated through eq 8[42,45] from the time series in Figure 5c,

$$\phi_i(t) = 2\pi\frac{t - t_k}{t_{k+1} - t_k} + 2k\pi \quad t_k < t < t_{k+1} \tag{8}$$

where t_k is the time of the kth peak of the oscillatory time series of the oscillator i.

A diagonal trend of $\Delta\phi_{ij}$ in Figure 6a corresponds to a phase difference which is not constant over time, while horizontal trends indicate that both oscillators have the same period and oscillate with a constant phase difference. This latter situation represents a "phase lock" state (i.e., a coherent behavior of the elements constituting the couple). We observed that the phase difference started from 0 when the system was initially homogeneous and changed in time when the oscillators were completely decoupled. However, when the stirring rate was progressively increased, inducing a global communication, $\Delta\phi_{ij}$ approached a constant value until it locks on 2π (0) up to the end of the experiment. The jumps between 2π and 0 in the region around 2000 s depend on how $\Delta\phi_{ij}$ is calculated and are due to small fluctuations around the locking phase value. Anyway, it is evident how the coupled oscillators adjust their oscillation frequency until they reach a synchronized behavior upon the increasing of the stirring (communication) rate. The same dynamics were also observed for the oscillation period τ (Figure 6b), the latter being calculated as the difference between two subsequent maxima in the time series. The values were randomly distributed before the onset of stirring. By increasing the stirring rate, each lattice element adjusted its oscillation period at ~200 s. After synchronization, τ smoothly decreased for each and every oscillator until the oscillations stopped.

CONCLUSIONS

In this paper, we present a new class of catalysts for the BZ oscillating reaction, based on the sorption of the iron-complex ferroin on the surface of natural inorganic materials, namely 1:1 and 2:1 homoionic clays. Ca^{2+} saturated kaolinite was chosen as the prototypical matrix for its resistance in the acidic and oxidizing environment of the BZ reaction. Also other ion-

dx.doi.org/10.1021/jp5032724 | J. Phys. Chem. C 2014, 118, 24389–24396

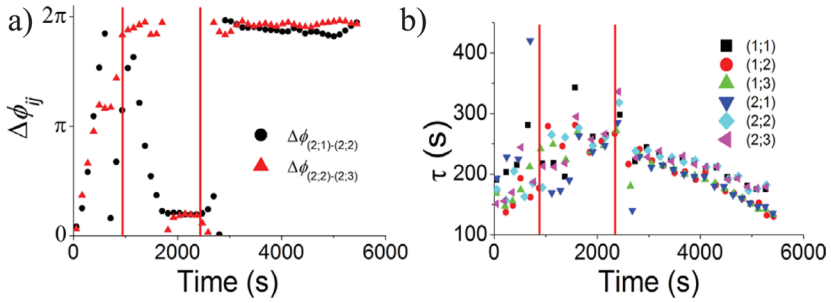

Figure 6. (a) Evolution in time of the phase difference between two couples of neighbor elements. (b) Evolution in time of the oscillation period of each element of the lattice. Vertical red lines in panels indicate the time at which stirring rate was varied, from zero to a low stirring rate (left bar) and finally to a high stirring rate (right bar).

saturated kaolinites and montmorillonites showed catalytic properties, though with a shorter lifespan. We proposed a simple procedure for the synthesis and regeneration of the Ferr-Kao catalytic microparticles, and we fully characterized the Ferr-Kao/BZ oscillating system. In particular, we found that Ferr-Kao induced the appearance of new features, such as an induction period in the global dynamics of the BZ reaction. Moreover, several oscillating parameters, like the amplitude and period, were affected by the presence of the catalytic clay particles. The experimental investigation of some of the BZ reaction subsystems, together with numerical simulations, proved that the characteristics of the system are due to a different reactivity of the new catalyst with respect to the ferroin complex; among these, a lower oxidation potential and the surface properties of the matrix (low local pH and sorption of organic substrates) seem to play a major role. In fact, we found the oscillation potential shifted toward higher values, meaning that the concentration of the oxidized form of the catalyst is the predominant species. The interaction of the clay surface with organic molecules and dicarboxylic acids, in particular, is known from the literature. Here we collected proofs that the interaction of MA and BrMA with the clay matrix is relevant for the appearance of the induction period and its length, and we calculated the equilibrium constant of the sorption process of the malonic acid onto the surface of the Ca-Kao substrate.

Catalytic microparticles can be used for applications where a network of discrete oscillators is required. The small size of the clay basic units (diameter < 2 μm) and their colloidal nature makes the Ferr-Kao particles interesting for the study of cooperative phenomena in networks of elements having dimensions at the border between the nano- and the mesoscale.[46] We employed Ferr-Kao to create a lattice of independent oscillators, each of them constituted by a homogeneous distribution of many particles. We then proved that a global coupling among the lattice elements, through the exchange of chemical intermediates, caused small adjustments of the phase and the period of single oscillators, which eventually led to a synchronous behavior of the whole system. Here we presented only an example of a small lattice, where the position of the stirring bar does not influence the synchronization dynamics of single oscillators. However, in larger lattices the distance from the stirring bar can be important in determining the local transport of the messenger molecules and more complex phase behaviors may exist. Finally, we showed that clays can act as suitable matrices for hosting and catalyzing chemical communication. Noteworthy, this model system has some aspects in common with prebiotic catalysis in minerals[16] and, therefore, with its related processes in the field of life origin.

■ ASSOCIATED CONTENT

Ⓢ Supporting Information

Further experimental procedures, characterization data for the new catalyst, and simulations details. This material is available free of charge via the Internet at http://pubs.acs.org.

■ AUTHOR INFORMATION

Corresponding Author

*E-mail: frossi@unisa.it.

Author Contributions

‖F.R. and O.L.P. contributed equally to this work.

Notes

The authors declare no competing financial interest.

■ ACKNOWLEDGMENTS

F.R. was supported by projects ORSA120144 and ORSA133584 funded by the University of Salerno (FARB ex 60%). Dr. Tonino Caruso from the University of Salerno is gratefully acknowledged for voltammetric measurements. Thanks are also due to Dr. Francesco D'Acapito (GILDA beamline ESRF Grenoble) for the XANES and EXAFS diagrams, Luigi Paolo D'Acqui at CNR-ISE (Institute of Ecosystem Study) for XRD pattern acquisition, and Ms. Ylenia Miele for experimental help.

■ REFERENCES

(1) Bosetto, M.; Arfaioli, P.; Pantani, O. L. *Clay Miner.* **2002**, *37*, 195−204.

(2) Muchaonyerwa, P.; Chevallier, T.; Pantani, O.; Nyamugafata, P.; Mpepereki, C.; Chenu, C. *Geoderma* **2006**, *133*, 244−257.

(3) Avisar, D.; Primor, O.; Gozlan, I.; Mamane, H. *Water, Air, Soil Pollut.* **2010**, *209*, 439−450.

(4) Choy, J.-H.; Choi, S.-J.; Oh, J.-M.; Park, T. *Appl. Clay Sci.* **2007**, *36*, 122−132.

(5) Murray, H. H. *Appl. Clay Sci.* **2000**, *17*, 207−221.

(6) Dinsmore, A. D.; Hsu, M. F.; Nikolaides, M. G.; Marquez, M.; Bausch, A. R.; Weitz, D. A. *Science* **2002**, *298*, 1006−1009.

(7) Shilpi, S.; Jain, A.; Gupta, Y.; Jain, S. *Crit. Rev. Ther. Drug Carrier Syst.* **2007**, *24*, 361−391.

(8) Subramaniam, A. B.; Wan, J.; Gopinath, A.; Stone, H. A. *Soft Matter* **2011**, *7*, 2600−2612.

(9) Dommersnes, P.; Rozynek, Z.; Mikkelsen, A.; Castberg, R.; Kjerstad, K.; Hersvik, K.; Otto Fossum, J. *Nat. Commun.* **2013**, *4*, 2066.

(10) Yamaguchi, T.; Suematsu, N.; Mahara, H. *Nonlinear Dynamics in Polymeric Systems*; ACS Symposium Series; 2004; Vol. *869*.

(11) Rossi, F.; Ristori, S.; Rustici, M.; Marchettini, N.; Tiezzi, E. *J. Theor. Biol.* **2008**, *255*, 404−412.
(12) Mikhailov, A. S.; Ertl, G. *ChemPhysChem* **2009**, *10*, 86−100.
(13) Rossi, F.; Liveri, M. L. T. *Ecol. Modell.* **2009**, *220*, 1857−1864.
(14) Epstein, I. R.; Vanag, V. K.; Balazs, A. C.; Kuksenok, O.; Dayal, P.; Bhattacharya, A. *Acc. Chem. Res.* **2011**, *45*, 2160−2168.
(15) Pietramellara, G.; Ascher, J.; Borgogni, F.; Ceccherini, M.; Guerri, G.; Nannipieri, P. *Biol. Fertil. Soils* **2009**, *45*, 219−235.
(16) Ruiz-Mirazo, K.; Briones, C.; de la Escosura, A. *Chem. Rev.* **2014**, *114*, 285−366.
(17) Maselko, J.; Reckley, J. S.; Showalter, K. *J. Phys. Chem.* **1989**, *93*, 2774−2780.
(18) Amemiya, T.; Nakaiwa, M.; Ohmori, T.; Yamaguchi, T. *Phys. D (Amsterdam, Neth.)* **1995**, *84*, 103−111.
(19) Das, I.; Pandey, V.; Rastogi, R. P.; Mishra, G. P. *Indian J. Chem., Sect. A: Inorg., Bio-inorg., Phys., Theor. Anal. Chem.* **2000**, *39*, 618−624.
(20) de Bussetti, S.; Ferreiro, E.; Helmy, A. *Clays Clay Miner.* **1980**, *28*, 149−154.
(21) Berkheiser, V.; Mortland, M. *Clays Clay Miner.* **1977**, *25*, 105−112.
(22) Liu, X.; Lu, X.; Wang, R.; Meijer, E. J.; Zhou, H. *Geochim. Cosmochim. Acta* **2011**, *75*, 4978−4986.
(23) Savitzky, A.; Golay, M. J. E. *Anal. Chem.* **1964**, *36*, 1627−1639.
(24) Smoes, M.-L. *J. Chem. Phys.* **1979**, *71*, 4669−4679.
(25) Taylor, A. F. *Prog. React. Kinet. Mech.* **2002**, *27*, 247−325.
(26) Rossi, F.; Rustici, M.; Rossi, C.; Tiezzi, E. *Int. J. Mol. Sci.* **2007**, *8*, 943−949.
(27) Rossi, F.; Simoncini, E.; Marchettini, N.; Tiezzi, E. *Chem. Phys. Lett.* **2009**, *470*, 147−150.
(28) Field, R. J.; Koros, E.; Noyes, R. M. *J. Am. Chem. Soc.* **1972**, *94*, 8649−8664.
(29) Tyson, J. J. *Frontiers in Mathematical Biology* **1994**, *100*, 569−587.
(30) Rossi, F.; Varsalona, R.; Liveri, M. L. T. *Chem. Phys. Lett.* **2008**, *463*, 378−382.
(31) Rossi, F.; Varsalona, R.; Marchettini, N.; Turco Liveri, M. L. *Soft Matter* **2011**, *7*, 9498.
(32) Specht, C. H.; Frimmel, F. H. *Phys. Chem. Chem. Phys.* **2001**, *3*, 5444−5449.
(33) Kang, S.; Xing, B. *Langmuir* **2007**, *23*, 7024−7031.
(34) Strahm, B. D.; Harrison, R. B. *Soil Sci. Soc. Am. J.* **2008**, *23*, 1653−1664.
(35) Kummer, U.; Hoops, S.; Sahle, S.; Gauges, R.; Lee, C.; Pahle, J.; Simus, N.; Singhal, M.; Xu, L.; Mendes, P. *Bioinformatics* **2006**, *22*, 3067−3074.
(36) Benini, O.; Cervellati, R.; Fetto, P. *Int. J. Chem. Kinet.* **1998**, *30*, 291−300.
(37) Koros, E.; Burger, M.; Friedrich, V.; Ladanyi, L.; Nagy, Z.; Orban, M. *Faraday Symp. Chem. Soc.* **1974**, *9*, 28−37.
(38) Toiya, M.; Gonzalez-Ochoa, H. O.; Vanag, V. K.; Fraden, S.; Epstein, I. R. *J. Phys. Chem. Lett.* **2010**, *1*, 1241−1246.
(39) Delgado, J.; Li, N.; Leda, M.; Gonzalez-Ochoa, H. O.; Fraden, S.; Epstein, I. R. *Soft Matter* **2011**, *7*, 3155.
(40) Tomasi, R.; Noel, J.-M.; Zenati, A.; Ristori, S.; Rossi, F.; Cabuil, V.; Kanoufi, F.; Abou-Hassan, A. *Chem. Sci.* **2014**, *5*, 1854−1859.
(41) Taylor, A. F.; Tinsley, M. R.; Wang, F.; Huang, Z.; Showalter, K. *Science* **2009**, *323*, 614−617.
(42) Fukuda, H.; Morimura, H.; Kai, S. *Phys. D (Amsterdam, Neth.)* **2005**, *205*, 80−86.
(43) Smith, M. L.; Heitfeld, K.; Slone, C.; Vaia, R. A. *Chem. Mater.* **2012**, *24*, 3074−3080.
(44) Tinsley, M.; Taylor, A.; Huang, Z.; Wang, F.; Showalter, K. *Phys. D (Amsterdam, Neth.)* **2010**, *239*, 785−790.
(45) Pikovsky, A. S.; Rosenblum, M. G.; Osipov, G. V.; Kurths, J. *Phys. D (Amsterdam, Neth.)* **1997**, *104*, 219−238.
(46) Ibele, M. E.; Lammert, P. E.; Crespi, V. H.; Sen, A. *ACS Nano* **2010**, *4*, 4845−4851.